



## Enhancement of visible light induced photocatalytic degradation of Eosin-Y by using TiO<sub>2</sub> and Ag doped TiO<sub>2</sub> nano catalyst

Sunil G. Shelar<sup>1,2</sup>, Vilas K. Mahajan<sup>2</sup>, Sandip P. Patil<sup>3</sup> and Gunvant H. Sonawane<sup>2,\*</sup>

<sup>1</sup>Department of Chemistry, S.R.N.D. Arts, Commerce and Science College, Bhadgaon, Dist. - Jalgaon- 424105 (M.S.) India

<sup>2</sup>Department of Chemistry, Kisan Arts, Commerce and Science College, Parola, Dist.- Jalgaon- 425111 (M.S.) India.

<sup>3</sup>Nano-chemistry Research Laboratory, G. T. Patil College, Nandurbar-425 412 (M.S.) India.

Received 24 Feb 2019,  
Revised 26 May 2019,  
Accepted 28 May 2019

### Keywords

- ✓ Eosin-Y,
- ✓ TiO<sub>2</sub> and Ag- doped TiO<sub>2</sub>,
- ✓ Photocatalysis,
- ✓ HR-LCMS,
- ✓ Kinetic Study.

[drgunvantsonawane@gmail.com](mailto:drgunvantsonawane@gmail.com)  
Phone: +912597222441;  
Fax: +912597223688

### Abstract

TiO<sub>2</sub> and Ag doped TiO<sub>2</sub> were synthesized by sol gel method. Morphology of as synthesized Ag doped TiO<sub>2</sub> nano catalyst was investigated using scanning electron microscopy (SEM), Electron dispersive X-ray spectroscopy (EDS) and X-ray diffraction (XRD). The photocatalytic activity of Ag doped TiO<sub>2</sub> nano catalyst was investigated by degradation of Eosin-Y solution under visible light radiation. The effects of various experimental parameters such as the Eosin-Y concentration, catalyst dose, and pH on the photocatalytic degradation were investigated. The kinetics study shows that the reaction follows first order kinetics. Among the different amounts of dopant that like 1, 2, and 4wt% Ag-doped with TiO<sub>2</sub> nanocatalyst. It was observed that 4 wt % Ag doped TiO<sub>2</sub> shows highest degradation with visible light radiation for Eosin-Y solution than pure TiO<sub>2</sub> nano catalyst. The particle size, morphology and separation of photo induced electron-hole pair are the main factors which influence photocatalytic activity. The degradation by-products formed during the complete degradation process were qualitatively identified by liquid chromatography-mass spectrometry (HR-LCMS) and a detailed degradation pathway has been proposed.

## 1. Introduction

The faster developments in the field of nanotechnology have stimulated considerable research efforts on the synthesis and manufacturing of novel devices for various high-technological potential applications [1,2]. Nanocrystalline titanium dioxide (TiO<sub>2</sub>) has many important applications such as: solar cells [3], photocatalytic splitting of water to hydrogen and oxygen [4], sensors [5], self-cleaning surfaces and degradation of environmental pollutants [6]. Due to the stability of modern dyes, conventional biological treatment methods for industrial wastewater are ineffective, resulting often in an intensively colored discharge from the treatment facilities. Recently, a number of researchers have dealt with heterogeneous Photocatalyst and Fenton based hybrid nanocatalyst for decomposition of many kinds of dyes [7-9] by UV, visible light and solar irradiation [10]. Shouair et al [11] reported plasmonic Au@TiO<sub>2</sub> photocatalyst bio-based chitosan fiber for the visible light induced photocatalysis of organic and inorganic pollutants. Photocatalytic performance of the TiO<sub>2</sub> can also improve by pulsed laser ablation in liquid [12,13]. Again adsorption capability of TiO<sub>2</sub> can be improved by decorating on eggshell nanocrystal [14]. In addition, titania has a relatively high band gap value of 3.2 eV. However for many applications it would be desirable to extend the band gap excitations towards the visible region, and also to prolong the lifetime of photogenerated charge carriers. Doping of titanium dioxide with transition metal like Pt, Au, Pd, Rh and Ag provides a relatively well-studied and convenient way of solving both problems described above. TiO<sub>2</sub> doped with transition metal ions can demonstrate extended band gaps and significantly higher photocatalytic efficiencies [15-19]. However among these transition metals only Ag is inexpensive so that its commercial applications are extended. The dopant concentration is an important parameter to be considered, as the amount of

dopant influences the processes of charge carrier trapping, separation, and recombination [20, 21]. Therefore, the amount of transition metal introduced should be within a so-called optimum concentration, as too low a dopant content does not affect the process of charge carrier generation and too high a content of doping metal results in the formation of extra recombination sites and shortens the lifetime of photo generated electrons and holes [22, 23]. Consequently, defining the optimum concentration of doping metal is a key factor for successful doping. This optimum value may vary significantly and depends on several factors, such as the type of dopant chosen, the coating deposition technique, annealing conditions, etc. [24].

Present study involves the synthesis of TiO<sub>2</sub> and Ag doped TiO<sub>2</sub> nano catalyst and characterization by SEM, EDS and XRD. Again optimum concentration of the Ag was reported. The effects of various parameters such as pH of dye solution, contact time, dose of the catalyst in photocatalytic degradation were studied. It also report the kinetics of degradation of Eosin-Y using TiO<sub>2</sub> and Ag doped TiO<sub>2</sub> nano catalyst.

## 2. Material and Methods

### 2.1. Material

Titanium tetra iso-propoxide (TTIP) was purchased from Sigma-Aldrich Pvt. Ltd., India, and aqueous ammonia (25%) Merck Specialties Pvt. Ltd. Silver nitrate and ethanol (99%) were obtained from Merck Ltd. The Eosin-Y dye was obtained from Loba Chemie Ltd. All chemicals used for synthesis of nano TiO<sub>2</sub> and Ag doped TiO<sub>2</sub> were of A.R. grade. Concentrations of the Eosin-Y were estimated using absorbance recorded on UV-VIS double beam spectrophotometer (Systronics model-2203) at the  $\lambda_{\max}$  500 nm. The pH was maintained using 0.1M NaOH and 0.1M HCl with pH meter (Equiptronics Model EQ-615).

### 2.2. Method

From stock solution of Eosin-Y, different concentrations were prepared in distilled water and the pH maintain at 8. The 50 ml Eosin-Y solution mixed with TiO<sub>2</sub> and Ag doped TiO<sub>2</sub> nano catalyst taken in the photocatalytic reactor. The solution was stirred and bubbled with molecular oxygen for 2 hours in the dark to allow equilibration of the system so that the loss of the compound due to adsorption can be taken into account. The dye sensitized TiO<sub>2</sub> and Ag doped TiO<sub>2</sub> was subjected to visible light irradiation using 500W Xenon lamp emitting 300-900nm visible light for the degradation of Eosin-Y. The catalyst was separated from the solution by centrifugation and the solution was analysed for determination of concentration of dye at  $\lambda_{\max}$  500 nm. The reaction kinetics was studied by varying different parameters like initial concentration of dye, catalyst dose and effect of pH on the Eosin-Y solution.

### 2.3. Synthesis of TiO<sub>2</sub> and Ag doped TiO<sub>2</sub>

The TiO<sub>2</sub> was synthesized by sol-gel technique using TTIP as precursor. TTIP-ethanol mixture (20 ml ethanol +5 ml TTIP) stirred for 10 minutes. Then 20 ml of deionised water was added drop wise for 20 minutes, after this 5ml aqueous ammonia was added and stirred for one hour and allowed for ageing for 12 hour after washing and drying the powder annealed at 450°C for one hour to get bare TiO<sub>2</sub> samples. The Ag-TiO<sub>2</sub> samples with 1% to 4% silver content were prepared by dissolving the required amount of silver nitrate in deionised water and added to homogeneous TTIP-ethanol solution drop wise followed by addition of aqueous ammonia in the solution under stirring for one hour. Then washed dried and calcinated at 450° C for one hour [25].

## 3. Results and discussion

### 3.1. SEM analysis

The SEM image of TiO<sub>2</sub> and Ag doped TiO<sub>2</sub> nano catalyst are shown in Figure 1 (a, b, c and d). The SEM image of TiO<sub>2</sub> and Ag doped TiO<sub>2</sub> nano catalyst shows spherical crystal structure having irregular size and shape. From Figure 1 it was observed that as the doping concentration of Ag increases the particle size of the photocatalyst also increases.

### 3.2. EDS analysis

The elemental analysis of material surface layer is obtained by electron dispersive X-ray spectroscopy (EDS). Figure 2 (a, b, c and d) shows that TiO<sub>2</sub> Ag doped TiO<sub>2</sub> nano catalyst contains only TiO<sub>2</sub> Ti K 80.70 %, O K 19.30 %. The 1 % Ag doped TiO<sub>2</sub> contains Ti K 67.90 %, O K 32.08 % and Ag 0.02 % , The 2 % Ag doped TiO<sub>2</sub> contains Ti K 79.61 %, O K 20.61 % and Ag 0.07 % . and the 4 % Ag doped TiO<sub>2</sub> contains Ti K 81.50 %, O K 18.29 % and Ag 0.21%. The EDS of TiO<sub>2</sub> and Ag doped TiO<sub>2</sub> indicates that as amount of dopant increases the percent Ag from EDS also increases. Thus micrograph proves existence of TiO<sub>2</sub> and Ag doped TiO<sub>2</sub> in the nanocatalyst.

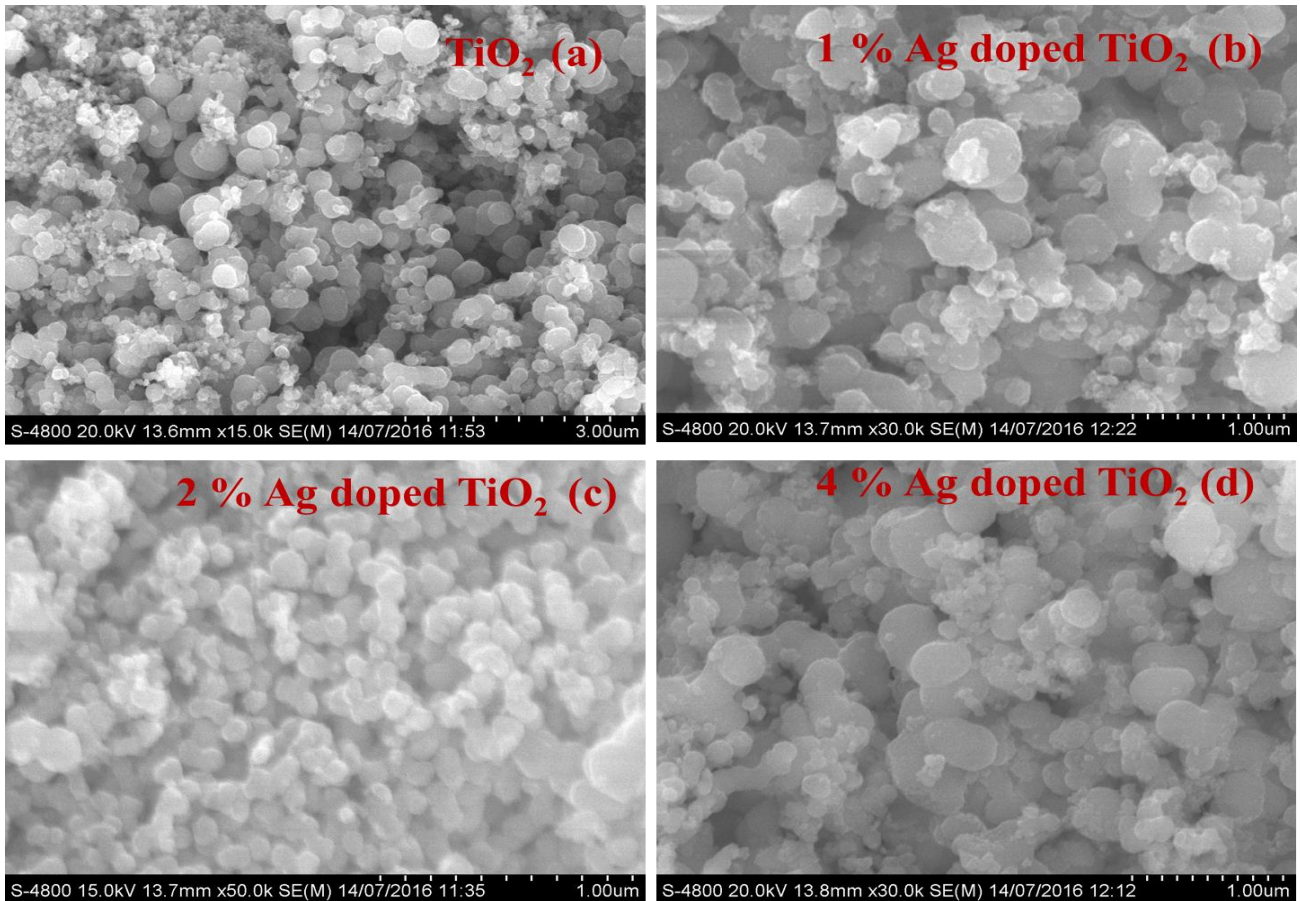


**Figure 1:** SEM images of a) TiO<sub>2</sub> b) 1% Ag doped TiO<sub>2</sub> c) 2% Ag doped TiO<sub>2</sub> d) 4% Ag doped TiO<sub>2</sub> nano catalysts.

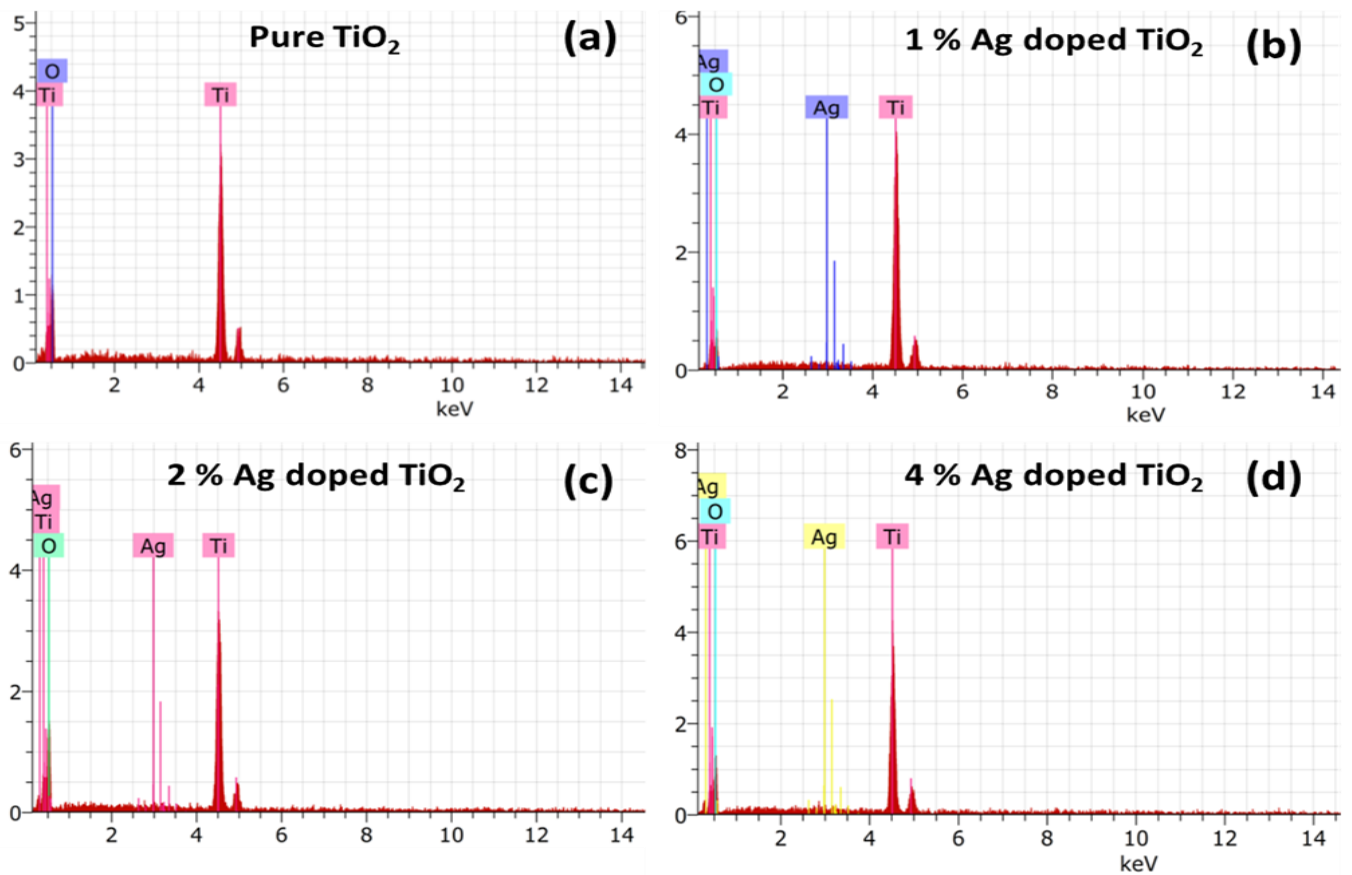


**Figure 2 :** The EDX spectrum of TiO<sub>2</sub> and Ag doped TiO<sub>2</sub> Nano catalyst.

### 3.3. X-ray diffraction analysis

The XRD patterns obtained for the TiO<sub>2</sub> and Ag doped TiO<sub>2</sub> are presented in Figure 3. It can be seen that both undoped and Ag doped TiO<sub>2</sub> were crystalline after annealing at 673.15 K in tetragonal structure. The major peaks in TiO<sub>2</sub> and Ag doped TiO<sub>2</sub> found that 25.29°, 48.09°, 54.0°, 55.20°, 62.70°, 68.90°, 70.40°, and 75.00° (JCPDS: 89- 4921).

### 3.4. Photocatalytic Study

#### 3.4.1. Effect of pH

The pH of dye solution largely influences the degradation rate [26]. Thus the influence of pH on photocatalytic degradation of Eosin-Y was performed and results obtained are shown in Figure 4. The natural pH of Eosin-Y is 8.4. The percentage degradation of Eosin-Y is lower in basic media that is increase in pH, the percentage degradation decreases and higher degradation is observed to acidic media. The pH 4 is suitable for degradation of Eosin-Y in presence of TiO<sub>2</sub> nano catalyst for photocatalytic degradation. This is because of pHzpc for TiO<sub>2</sub> is 5.1. Photocatalyst surface becomes positively charged below pHzpc (5.1) and above this pH, the surface is negatively charged due to adsorbed OH<sup>-</sup> ions. Hence pH lower than 5.1 favours adsorption and consequently photocatalytic degradation by electrostatic attraction among the positively charged photocatalyst and anions of the Eosin-Y [27,28].

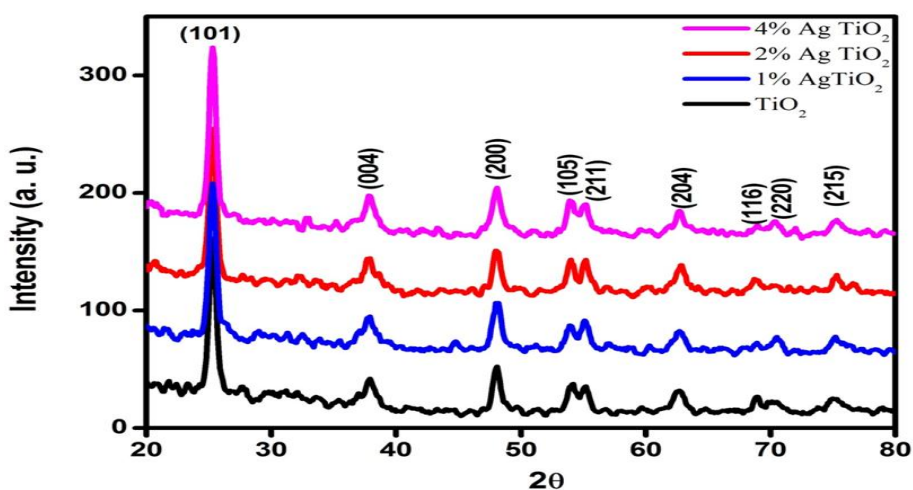


Figure 3: XRD of pure and Ag doped TiO<sub>2</sub>.

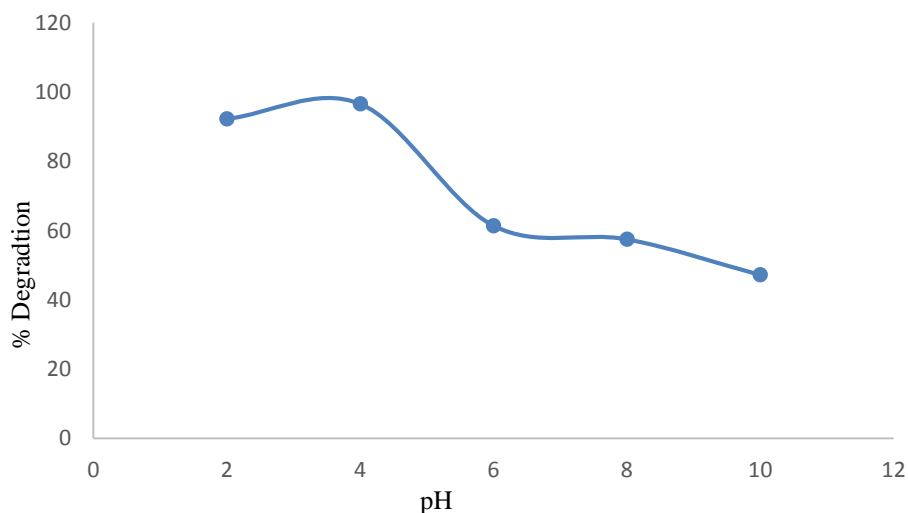
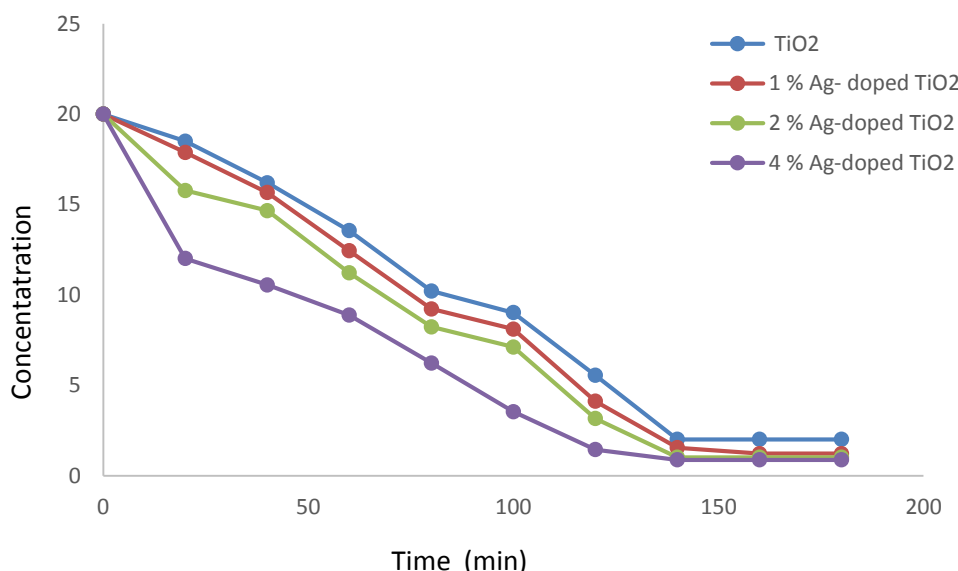


Figure 4: Effect of pH on photocatalytic degradation of Eosin-Y (Conc. 10 mg/L, catalyst dose 1.0 g/L and reaction time 120 min).

### 3.4.2. Effect of catalyst on Dye Degradation

The effect of catalyst on initial dye concentration of Eosin-Y was investigated by changing the doping amount Ag in TiO<sub>2</sub> as 1%, 2% and 4% using 2 g/L of TiO<sub>2</sub> and Ag doped TiO<sub>2</sub> nano catalyst at pH 4. The results showed that dye concentration decreases from 20 mg/L to 2.01 mg/L with increasing in doping concentrations from TiO<sub>2</sub>, 1 % Ag doped TiO<sub>2</sub> 20 mg/L to 1.22 mg/L, 2% Ag doped TiO<sub>2</sub> 20 mg/L to 1.02 mg/L, 4% Ag doped TiO<sub>2</sub> 20 mg/L to 0.88 mg/L, (Figure 5). This was due to the reason that as doping concentration increased the concentration of unabsorbed dye in the solution decreases which lead to more penetration of light through the solution on to the surface of TiO<sub>2</sub> and Ag doped TiO<sub>2</sub> thereby increase the concentration of •OH radicals on the surface and hence increases the percentage degradation [29].



**Figure 5:** Effect of catalyst type on initial dye concentration (Eosin-Y 10 mg/L, pH 4, Catalyst dose 1.0 g/L, reaction time 180 min.)

### 3.4.3. Effect of catalyst Dose

To avoid the excessive use of catalyst, the optimum dose was determined using concentrations of TiO<sub>2</sub> under UV light. It was found that rate of degradation initially increases with the increase in catalyst dose, but beyond a certain level it remained almost constant. From Figure 6 it is observed that after 1g/L of catalyst dose percent degradation remains almost constant so in present case 1g/L was found to be the optimum catalyst concentration [30].

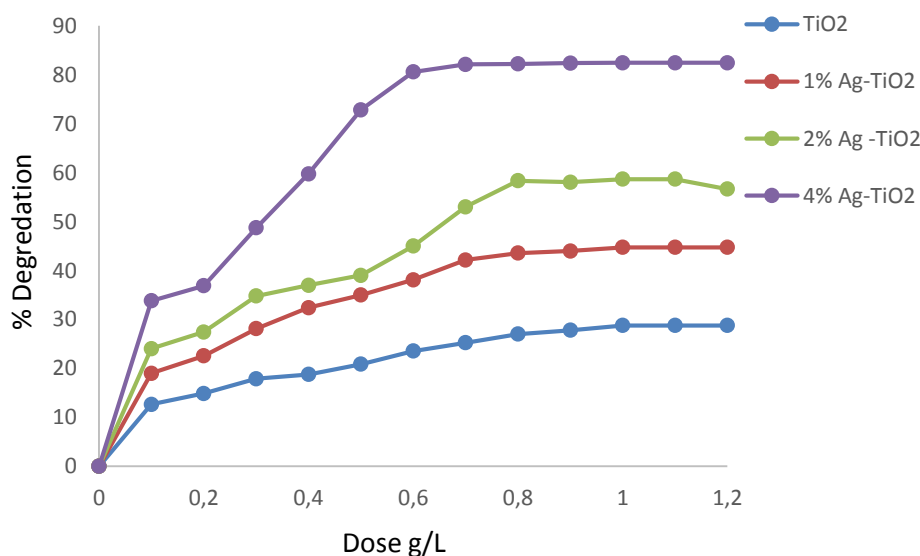


**Figure 6:** Effect of catalyst dose on percentage degradation of Eosin Y (pH 4, Eosin Y conc. 40 mg/L and reaction time 120 min.)

The increase in catalysts concentration has a positive influence on the number of photons absorbed and number of dye molecules adsorbed. This in turns enhances the rate of dye degradation. Above a certain catalysts concentration the numbers of substrate molecules are not sufficient to fill the surface active sites of TiO<sub>2</sub>. Hence, further addition of catalyst does not lead to the enhancement of degradation rate. This is may be due to the reduction in the penetration of light with surplus amount of TiO<sub>2</sub>. The surplus addition of the catalyst makes the solution more turbid and light penetration is hindered from the sample [31, 32].

#### 3.4.4. Effect of doping percentage

Figure 7 shows that the effect of different doping ratios on the photocatalytic degradation of Eosin-Y. The values of catalyst dosage 1 g/L, pH 4 and the concentration of Eosin-Y were 20 mg/L, respectively. As shown in Figure 7, during the contact time, the Eosin-Y degradation efficiency (%) was increased slightly with the increase of doping ratio from 1 to 4 %. Photocatalytic activity of doping concentration increases with decreasing the band gap energy [33]. In addition, rapid transfer of the electrons from the TiO<sub>2</sub> to the Ag may improve the photocatalytic activity and increase the efficiency of photodegradation [34].

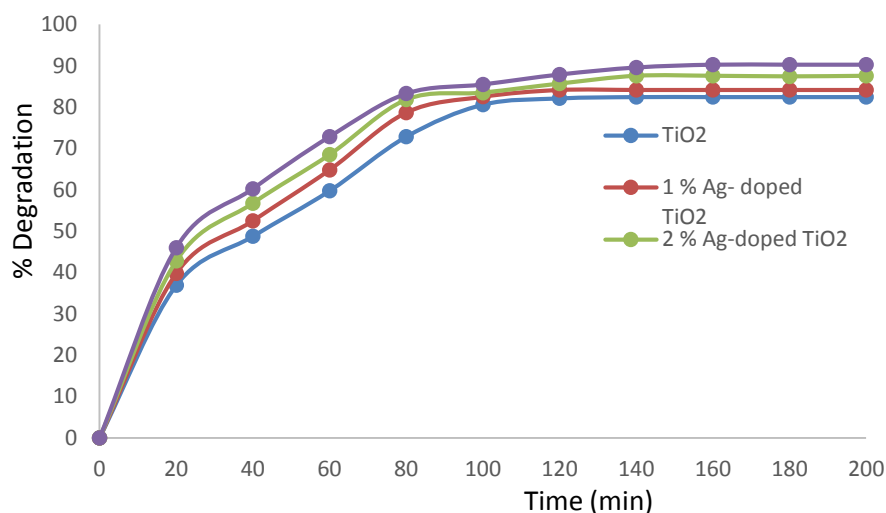


**Figure 7:** Effect of doping proportion on percentage degradation of Eosin Y (undoped TiO<sub>2</sub>, 1% Ag doped TiO<sub>2</sub>, 2% Ag doped TiO<sub>2</sub> and 4% Ag doped TiO<sub>2</sub> 1.0 g/L, pH 4 Eosin-Y conc. 40 mg/L and reaction time 200 min.)

#### 3.4.5. Effect of initial dye concentration

The effect of initial dye concentration on photocatalytic degradation of Eosin-Y was studied by varying the dye concentration from 10 to 40 mg/L (Figure 8) at fixed catalyst concentration. It can be observed that, as the dye concentration increases percent degradation decreases.

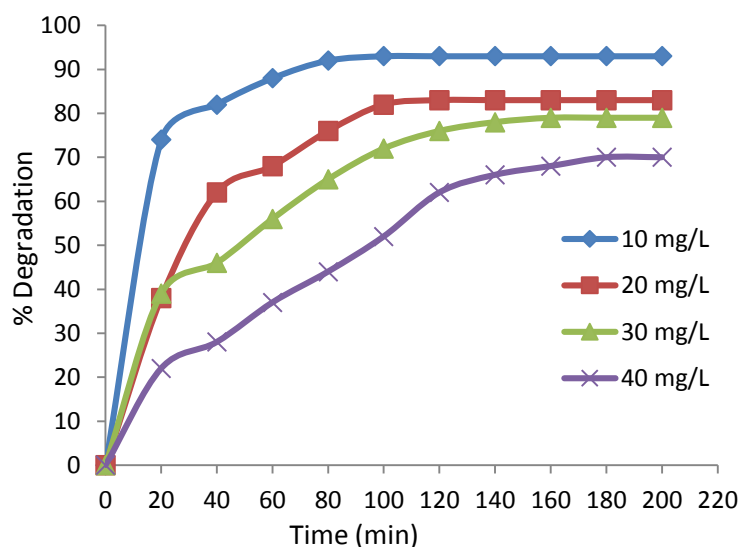


**Figure 7:** Effect of doping proportion on percentage degradation of Eosin Y (undoped TiO<sub>2</sub>, 1% Ag doped TiO<sub>2</sub>, 2% Ag doped TiO<sub>2</sub> and 4% Ag doped TiO<sub>2</sub> 1.0 g/L, pH 4 Eosin-Y conc. 40 mg/L and reaction time 200 min.)

As the concentration of dye increases the color of solution becomes more intense due to more dye molecules which alters the light to reach the catalyst surface to produce active species responsible for degradation and thereby decreases the degradation efficiency of catalyst and secondly, less number of active site of catalyst is available due increase in adsorption which also lowers the catalyst efficiency.

### 3.4.6. Kinetics of degradation

The photocatalytic degradation of Eosin-Y by TiO<sub>2</sub> nano catalyst obeys pseudo-first-order kinetics:

$$-dC/dt = k_{app}C \quad (1)$$

Integration of the above equation (with the restriction of  $C=C_{ads}$  at  $t=0$ , with  $C_{ads}$  being the initial concentration in the bulk solution after dark adsorption and  $t$  the reaction time) leads to the following expected relation [35]:

$$-\ln(C_0/C) = k_{app}t \quad (2)$$

Where  $C$  and  $C_0$  are the reactant concentration at time  $t = t$  and  $t = 0$ , respectively, and  $k_{app}$  and  $t$  are the apparent reaction rate constant and time, respectively. According to the equation, a plot of  $-\ln(C_0/C)$  versus  $t$  will yield a slope of  $k_{app}$ . The results are displayed in Figure 9. The linearity of the plot suggests that the photocatalytic degradation reaction approximately follows pseudo-first-order kinetics with  $k_{app}$  of 0.044 min<sup>-1</sup>, 0.986 min<sup>-1</sup>, 0.980 min<sup>-1</sup> and 0.987 min<sup>-1</sup> for TiO<sub>2</sub>, 1% Ag doped TiO<sub>2</sub> photocatalyst, 2% Ag Doped TiO<sub>2</sub> photocatalyst, 4% Ag Doped TiO<sub>2</sub> photocatalyst, respectively.

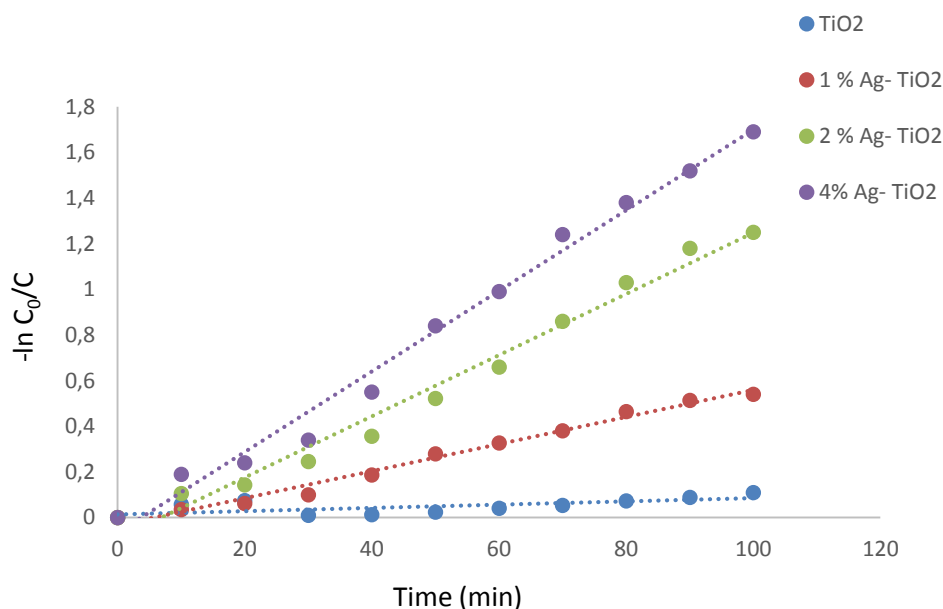


**Figure 9:** First order kinetics plot of Eosin-Y degradation under TiO<sub>2</sub>, 1% Ag doped TiO<sub>2</sub> photocatalyst, 2% Ag doped TiO<sub>2</sub> photocatalyst, 4% Ag doped TiO<sub>2</sub> photocatalyst (Eosin-Y conc. 20 mg/L, TiO<sub>2</sub> 1 g/L, pH 4, and reaction time 100 min.)

### 3.4.7. Recycle performance of Ag doped TiO<sub>2</sub> nanocatalyst

The stability, efficiency and reusability plays important role in the effectiveness of the process towards the removal of the dye from aqueous solution [36]. To find out the stability and efficiency of Ag doped TiO<sub>2</sub> nanocatalyst as well as cost effectiveness of the process, the reusability of Ag doped TiO<sub>2</sub> nanocatalyst was investigated for the degradation of Eosin-Y under UV radiation. To study its reusability, the powdered nanocatalyst was centrifuged after completion of each photocatalytic experiment. The recovered sample was reused for 3 times under same experimental conditions. The results obtained are shown in Figure 10. It shows that % degradation of Eosin-Y by Ag doped TiO<sub>2</sub> nanocatalyst after 1<sup>st</sup> run achieved up to 88.75% (100 min). At the end of 4<sup>th</sup> cycle it decreases down to 87.08%. The catalytic activity was found to decrease slightly after 4<sup>th</sup> cycle. This decrease may be due to, i) loss of reused catalyst during sampling every time, and ii) irreversible changes that are brought about by pollutants on the photocatalyst surface. From Figure 10 it was clear that Ag doped TiO<sub>2</sub> have excellent stability and it does not undergo corrosion during photocatalytic degradation.

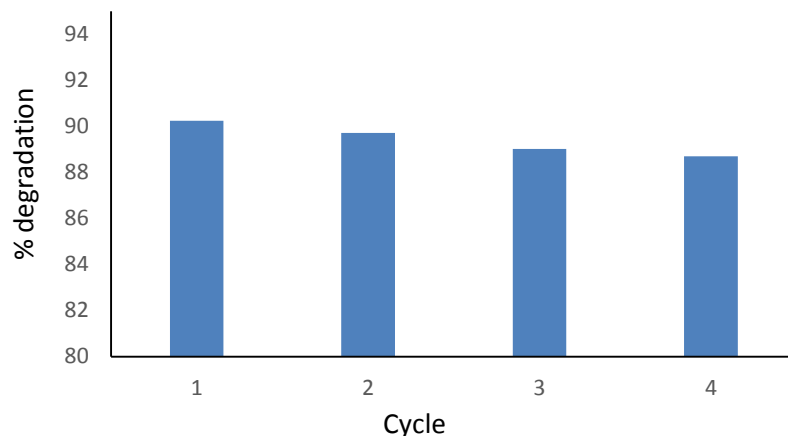


**Figure 9:** Reusability study of Ag doped TiO<sub>2</sub> nano catalyst.

### 3.4.8. Scavenging Study

AOP involving heterogeneous photocatalysis explains the mechanism of Eosin-Y degradation. This process involves generation of e<sup>-</sup>-hole pair. This photogenerated e<sup>-</sup>-hole pair again generates highly reactive O<sub>2</sub><sup>-•</sup> and •OH radicals in subsequent steps which are responsible for oxidative mineralization of the dye [37, 38]. Also there is generation of hydrogen atoms from water, causing reduction of the dye [39, 40]. It is necessary to detect main active species in the photocatalysis for elucidation of photocatalytic degradation mechanism of Eosin-Y by TiO<sub>2</sub>. It can be possible by scavenging study performed under identical conditions upon addition of scavenger into the dye solution during photocatalysis. The oxidative species like •OH, h<sup>+</sup> and O<sub>2</sub><sup>-•</sup> are trapped by using isopropanol (i-PrOH), methanol (MeOH), ethylene diamine tetraacetic acid (EDTA) and Potassium iodide (KI). These are used as •OH scavenger, O<sub>2</sub><sup>-•</sup> scavenger, h<sup>+</sup> scavenger, and •OH & h<sup>+</sup> scavenger respectively. Smaller alcohols like i-PrOH also undergoes direct oxidation due to the photo-generated holes. But the extent is negligible, thus neglected. The results in terms of Eosin-Y degradation by TiO<sub>2</sub> with and without scavengers are summarized in Figure 11. Upon addition of MeOH, EDTA, i-PrOH and KI; the photocatalytic degradation of Eosin-Y decreases down to 72.33, 61.32, 33.65, and 29.46% respectively as compared to photocatalytic degradation carried out in aqueous medium (90.25%). From Figure 10 it was clear that, MeOH has very little influence on Eosin-Y degradation. However, the photocatalytic performance of TiO<sub>2</sub> greatly depressed due to addition of •OH and h<sup>+</sup> scavenger i.e. KI, suggesting that the photo-generated holes and •OH are the predominant species of TiO<sub>2</sub> whereas, the O<sub>2</sub><sup>-•</sup> radical plays supportive role in the degradation of Eosin-Y.

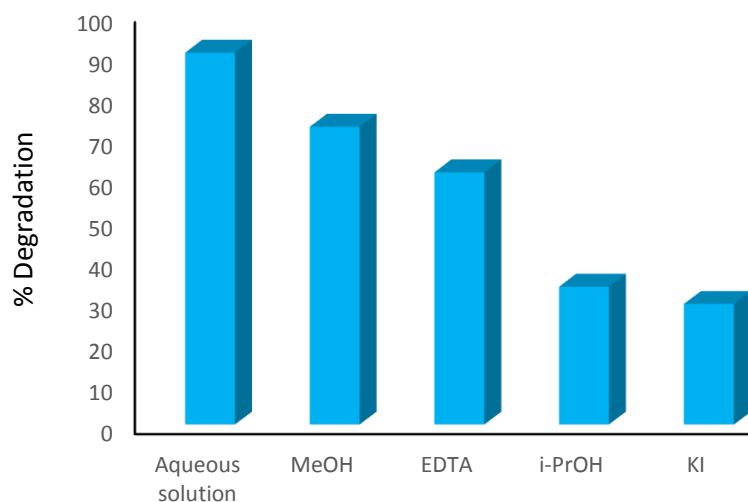


**Figure 11:** Photocatalytic degradation of Eosin Y TiO<sub>2</sub> with and without scavenger.

### 3.4.9. Degradation Mechanism

The non-selective nature of the reaction between the radicals and organic pollutants leads to the formation of number of products in the AOPs. LCMS was used to identify the intermediates produced during the degradation process. The structures of degraded products are assigned on the basis of analysis of molecular ion peaks and their corresponding fragmentation patterns. The probable degradation pathway of Eosin-Y is shown in Figure 11. The Figure 12 indicates that Eosin-Y undergoes debromination, decarboxylation followed by ring opening, and addition of  $\bullet\text{OH}$  radicals generated from AOP. Then Eosin-Y subsequently degraded into  $\text{CO}_2$  and  $\text{H}_2\text{O}$ .

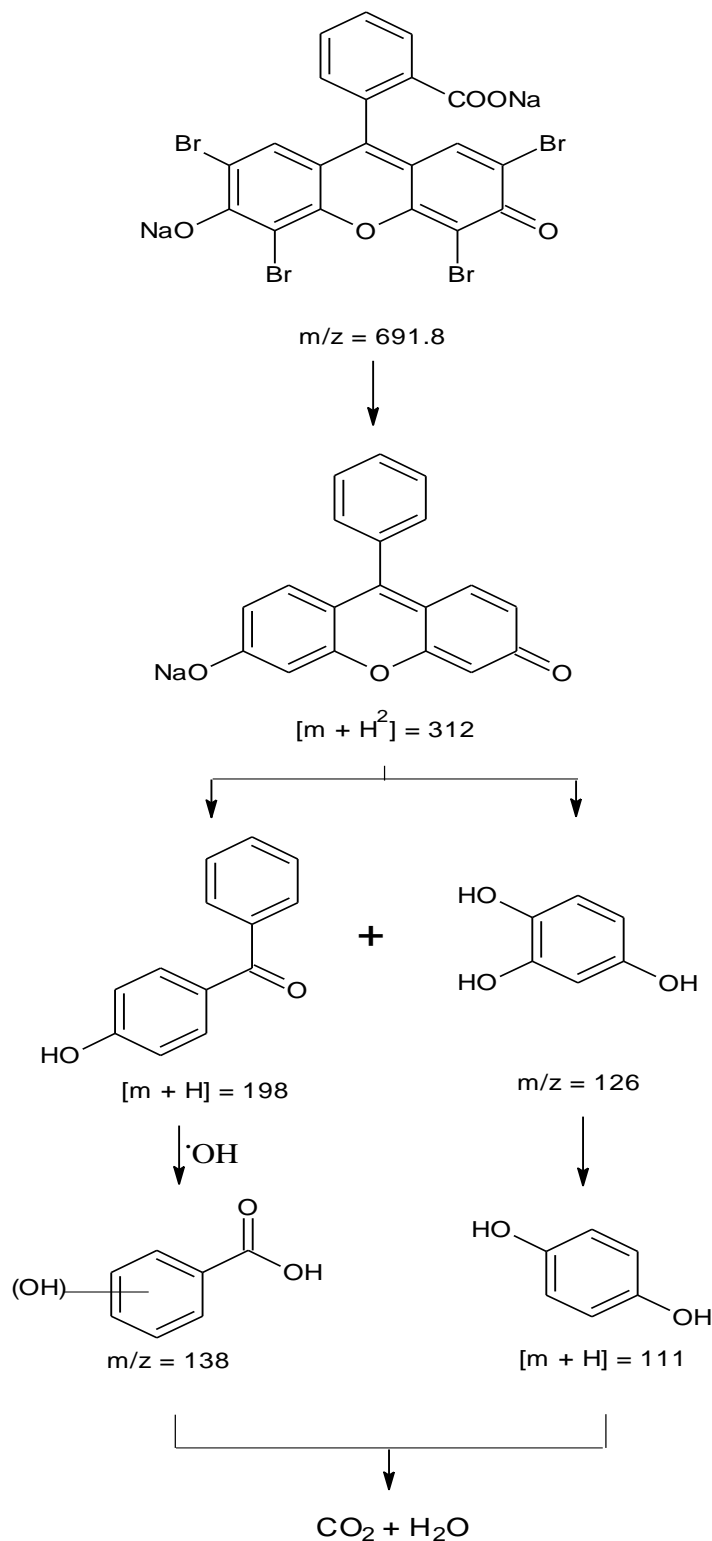


**Figure 12:** The possible reaction intermediates formed during photocatalytic degradation of Eosin-Y using  $\text{TiO}_2$  and Ag doped  $\text{TiO}_2$  nano catalyst.

## Conclusion

The photocatalytic degradation of Eosin-Y in the presence of nano TiO<sub>2</sub> and nano Ag-doped TiO<sub>2</sub> were show promising results towards removal of Eosin-Y. The photocatalytic degradation followed first order kinetics with respect to Eosin-Y. The percentage degradation of dye increased with an increase in catalyst loading and decrease with increase in pH, initial concentration of dye. The pH 4 found to be suitable for photocatalytic degradation of Eosin-Y. A comparative study shows that 4 % Ag doped TiO<sub>2</sub> photocatalyst is effective than bareTiO<sub>2</sub>, 1 % Ag doped TiO<sub>2</sub>, 2% Ag doped TiO<sub>2</sub> for photocatalytic degradation of Eosin-Y. The HR-LCMS analysis clearly indicates the non-generation of secondary waste after degradation of Eosin-Y by Ag doped TiO<sub>2</sub> nano catalyst. This reveals the potential use of the photocatalyst on industrial scale.

## Acknowledgements

The authors have gratefully acknowledged to Central Instrumentation Centre, University Institute of Chemical Technology, NMU Jalgaon for SEM, EDX and Department of Physics, Savitribai Phule Pune University, Pune for XRD analysis. The authors also thankful to Principal, Kisan Arts, Commerce and Science College, Parola, Dist. Jalgaon (M.S.) for providing necessary laboratory facilities and Principal, S.R.N.D. Arts, Commerce and Science College, Bhadgaon Dist. Jalgaon (M.S.) for providing necessary help for the work.

## References

1. M. Bordbar, S. Mohammad Vasegh, S. Jafaric, A. Yeganeh, Faal, *Iranian J. Catal.* 5 (2015) 135-141.
2. H. S. EL-Sheshtawy, H. M. El-Hosainy, K. R. Shouir, I. M. El-Mehasseb, M.El-Kemary, *Applied Surface Science* 467(2019) 268-276.
3. Ch. Girginov, P. Stefchev, P. Vitanov, Hr. Dikov, *J. Eng. Sci. Technol. Review* 5 (2012) 14 – 17.
4. L. Cao, R. Li, *Short-Term Wind Speed Forecasting Model for Wind Farm Based on Wavelet Decomposition*, DRPT 2008, 6- 9 April, Nanjing China, 2525-2529.
5. R. M. Rao, A. S. Bopardikar, *Wavelet Transforms*, Pearson Education, Low Price Edition, 2005.
6. R. Leary, A. Westwood, *Carbon* 49 (2011) 741–772.
7. V. Augugliaro, C. Baiocchi, A. Bianco Prevot, E. García-López, V. Loddo, S. Malato, G. Marci, L. Palmisano, M. Pazzi, E. Pramauro, *Chemosphere* 49 (2002) 1223–1230.
8. R. Datta, V.T. Ranganathan, *IEEE Trans. Energy Convers.* 17 (2002) 414-421.
9. K. Shoueir, H El-Sheshtawy, M Misbah, H. El-Hosainy, I. El-Mehasseb, M. El-Kemary, *Carbohydrate polymers* 197 (2018) 17-28.
10. Z. Sartep, A. E. Pirbazari, M. A. Aroon, *J. Water Environ. Nanotechnol.* 1 (2016) 135-144.
11. K. Shoueir, S. Kandil, H. El-hosainy, M. El-Kemary, *Journal of Cleaner Production* 230 (2019) 383-393.
12. A. Balati , S. Tek, K. Nash, H. Shipley, *J. Colloid Interface Sci.* 541 (2019) 234–248.
13. A. Balati, D. Wagle, K. L. Nash, H. J. Shipley, *Applied Nanoscience* 9 (2019)19-32.
14. M. A. El-Kemary, I. M. El-mehasseb, K. R. Shoueir, S.E. El-Shafey, O. I. El-Shafey, H. A. Aljohani, R. R. Fouad J. Dispersion Sci. Technol. 39 (2018) 911-921.
15. M. Ratova, P.J. Kelly, G.T.West, I. Iordanova, *Surf. Coat. Technol.* 228 (2013) S544–S549.
16. N. Farahani, P.J. Kelly, G. West, M. Ratova, C. Hill, V. Vishnyakov, *Thin Solid Films* 520 (2011) 1464–1469.
17. S. I. Mogal, V. G. Gandhi, M. Mishra, S. Tripathi, T. Shripathi, P. A. Joshi, D. O. Shah, *Ind. Eng. Chem. Res.* 53 (2014) 5749–5758.
18. M. Abdennouri, A. Elhalil, M. Farnane, H. Tounsadi, F.Z. Mahjoubi, R. Elmoubarki, M. Sadiq, L. Khamar, A. Galadi, M. Baalala, M. Bensitel, Y. El hafiane, A. Smith, N. Barka, *J. Saudi Chem. Soc.* 19(2015) 485–493.
19. A. Pandey, S. Kalal, C. Ameta, R. Ameta, S. Kumar, P. B. Punjabi, *J. Saudi Chem. Soc.* 19 (2015) 528–536.
20. M. Yao, J. Chen, C. Zhao, Y. Chen, *Thin Solid Films* 517 (2009) 5994–5999.
21. O. Avciata, Y. Benli, S. Gorduk, O. Koyun, *J. Eng. Tech. Applied Sci.* 1 (2016) 1-12.
22. H. Su, Y.-T. Huang, Y.-H. Chang, P. Zhai, Nga Yu Hau, P. C. H. Cheung, W.-T. Yeh, T.-C. Wei, S.-P. Feng, *Electrochim. Acta* 182 (2015) 230–237.

23. M. B. Suwarnkar, G. V. Khade, S. B. Babar, K. M. Garadkar, *J. Mater. Sci.- Mater. Electron.* 28 (2017) 17140–17147.
24. O. Lorret, D. Francová, G. Waldner, N. Stelzer, *Appl. Catal. B Environ.* 91 (2009) 39–46.
25. H. Ninsonti, W. Chomkitichai, A. Baba, K. Shinbo, K. Kato, F. Kaneko, N. Wetchakun, S. Phanichphant, *Int. Sci. J.: Env. Sci.* 3 (3) (2014).
26. S. Tanaka, U.K. Saha, *Water Sci. Technol.* 30 (1994) 47-57.
27. A. Akyol, H. C. Yatmaz, M. Bayramoglu, *Appl. Catal. B* 54 (2004) 19–24.
28. S. P. Patil, V. K. Mahajan, V. S. Shrivastava, G. H. Sonawane, *Iran. Chem. Commun.* 5 (2017) 417-428.
29. V. K. Mahajan, G. H. Sonawane, *J. Applicable Chem.* 4 (2015) 1500-1506.
30. T. Sreethawong, S. Ngamsinlapasathian, S. Yoshikawa, *Mater. Lett.* 78 (2012) 135–138.
31. S. Kaur, V. Singh, *Ultrason. Sonochem.* 14 (2007) 531-37.
32. A. P. Toor, A. Verma, C. K. Jotshi, P. K. Bajpai, V. Singh, *Dyes Pigm.* 68, (2006) 53-60.
33. A.R. Khataee, R.D. C. Soltani, A. Karimi, S.W. Joo, *Ultrason. Sonochem.* 23 (2015) 219–230.
34. S. Rengaraj, X.Z. Li, *J. Mol. Catal. A* 243 (2006) 60–67.
35. V. K. Mahajan, S. P. Patil, S. H. Sonawane, G. H. Sonawane, *AIMS Biophysics*, 3 (3) (2016) 415-430.
36. K. Prakash, P.S. Senthilkumar, P. Latha, K.S. Durai, R. Shanmugam, S. Karuthapandian, *Mater. Res. Bull.* 93 (2017) 112-122.
37. H. Park, W. Choi, *J. Phys. Chem. B* 108 (2004) 4086–4093.
38. D. Zhang, R. Qiu, L. Song, B. Eric, Y. Mo, X. Huang, *J. Hazard. Mater.* 163 (2009) 843–847.
39. S. Meshram, R. Limaye, S. Ghodke, S. Nigam, S. Sonawane, R. Chikate, *Chem. Eng. J.* 172 (2011) 1008–1015.
40. S. P. Patil, R.P. Patil, V.K. Mahajan, G.H. Sonawane, V.S. Shrivastava, S. Sonawane, *Mater. Sci. Semicond. Process.* 52 (2016) 55–61.

(2019) ; <http://www.jmaterenvironsci.com>